LETTER

https://doi.org/10.1038/s41586-019-1257-5

Cas13–induced cellular dormancy prevents the rise of CRISPR–resistant bacteriophage

Alexander J. Meeske[1]*, Sandra Nakandakari-Higa[1] & Luciano A. Marraffini[1,2]*

Clustered, regularly interspaced, short palindromic repeat (CRISPR) loci in prokaryotes are composed of 30–40-base-pair repeats separated by equally short sequences of plasmid and bacteriophage origin known as spacers[1–3]. These loci are transcribed and processed into short CRISPR RNAs (crRNAs) that are used as guides by CRISPR-associated (Cas) nucleases to recognize and destroy complementary sequences (known as protospacers) in foreign nucleic acids[4,5]. In contrast to most Cas nucleases, which destroy invader DNA[4–7], the type VI effector nuclease Cas13 uses RNA guides to locate complementary transcripts and catalyse both sequence-specific *cis*- and non-specific *trans*-RNA cleavage[8]. Although it has been hypothesized that Cas13 naturally defends against RNA phages[8], type VI spacer sequences have exclusively been found to match the genomes of double-stranded DNA phages[9,10], suggesting that Cas13 can provide immunity against these invaders. However, whether and how Cas13 uses its *cis*- and/or *trans*-RNA cleavage activities to defend against double-stranded DNA phages is not understood. Here we show that *trans*-cleavage of transcripts halts the growth of the host cell and is sufficient to abort the infectious cycle. This depletes the phage population and provides herd immunity to uninfected bacteria. Phages that harbour target mutations, which easily evade DNA-targeting CRISPR systems[11–13], are also neutralized when Cas13 is activated by wild-type phages. Thus, by acting on the host rather than directly targeting the virus, type VI CRISPR systems not only provide robust defence against DNA phages but also prevent outbreaks of CRISPR-resistant phage.

We investigated the ability of Cas13a to provide phage resistance to *Listeria*, a natural host for the type VI-A CRISPR–Cas system, which we previously established as a model to study immunity against plasmid transfer[14]. We constructed *Listeria ivanovii* ΩCRISPR^{VI}, a strain that is susceptible to infection by the phage ϕRR4 and carries the type VI-A CRISPR locus of *Listeria seeligeri* ATCC35967 (Extended Data Fig. 1a–c). To study Cas13a-mediated phage immunity, we generated a spacer library containing 41,276 unique ϕRR4 sequences, tiled every two nucleotides across both strands of the phage genome (Supplementary Information 1). We introduced the spacer library into *L. ivanovii* ΩCRISPR^{VI} and infected the cells with ϕRR4. We collected intact cells before and five hours after infection, and used next-generation sequencing to determine spacer abundance. Wild-type *L. ivanovii* RR3 cells decreased in optical density at 600 nm (OD_{600}) after infection, but the diverse set of spacers in the library provided protection from lysis (Extended Data Fig. 1d). We calculated enrichment ratios for each spacer as the read count after infection divided by the number of initial reads. The observed enrichment ratios were modest, consistent with previously reported growth defects associated with Cas13a activation[8,14]. As expected, given the fact that Cas13a targets RNA, we found a strong strand bias in spacer efficacy: spacers that generate a crRNA complementary to predicted transcripts (based on open reading frame direction) showed substantially higher enrichment ratios than those for which there should not be a target transcript (Fig. 1a, b, Extended Data Fig. 1e, Supplementary Information 1). To confirm this, we performed RNA sequencing (RNA-seq) analysis of phage-infected cells (Extended Data Fig. 2a) and found a strong correlation between protospacer transcription and the protection conferred by the corresponding spacer (Fig. 1c, Extended Data Fig. 1b, Extended Data Fig. 2b, Supplementary Information 1). We selected three individual spacers from the library for further characterization: *spcA*, which targets the ϕRR4 anti-CRISPR region; *spcE*, which targets the early lytic genes; and *spcL*, which targets the late lytic genes (Extended Data Fig. 1a). Each spacer strongly reduced both the efficiency of infective centre formation (Fig. 1d) and the phage burst size (Fig. 1e). Together, these results show that Cas13a uses crRNAs complementary to phage transcripts to prevent the establishment and maintenance of infection.

The experiments described above demonstrated that, although different individual spacer sequences supported different levels of defence, spacers that matched either essential or non-essential transcripts (such as those produced by phage anti-CRISPR genes, see below), and early- or late-expressed RNAs, could mediate a robust defence. This indicates

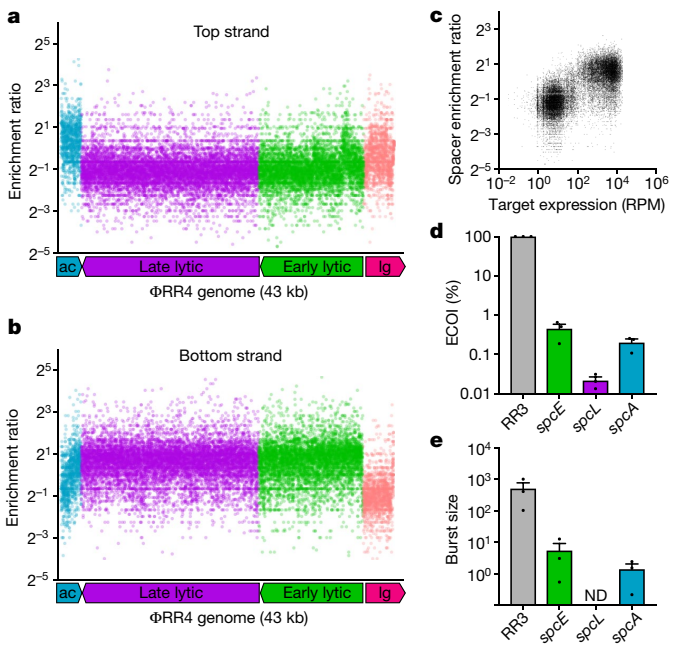

Fig. 1 | Cas13a halts DNA phage infection upon protospacer transcription. a, **b**, Enrichment of spacers targeting the top (**a**) or bottom (**b**) strands of the ϕRR4 genome after phage exposure, plotted by position. ac, anti-CRISPR; lg, lysogeny. **c**, Correlation of target transcript expression (RPM, reads per million mapped reads) and enrichment of the corresponding spacer. **d**, Mean (± s.e.m.) efficiency of ϕRR4 infective centre formation (ECOI, efficiency of centre of infection; $n = 3$ biological replicates) on a strain lacking CRISPR (RR3) or ΩCRISPR^{VI} strains programmed with *spcE*, *spcL* or *spcA*. **e**, Mean (± s.e.m.) ϕRR4 burst size for the strains tested in **d** ($n = 3$ biological replicates). ND, not detectable.

[1]Laboratory of Bacteriology, The Rockefeller University, New York, NY, USA. [2]Howard Hughes Medical Institute, The Rockefeller University, New York, NY, USA. *e-mail: ameeske@rockefeller.edu; marraffini@rockefeller.edu

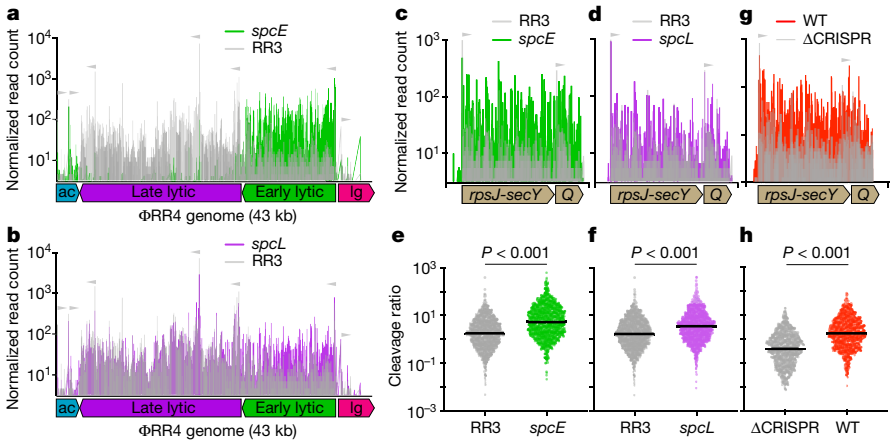

Fig. 2 | Cas13a elicits widespread cleavage of host and phage transcripts. a–d, RNA 5′ end mapping of ϕRR4 (**a**, **b**) or *rpsJ-secY-rplQ* (**c**, **d**) transcripts after infection of *L. ivanovii* RR3 or ΩCRISPR^{VI} strains programmed with *spcE* (**a**, **c**) or *spcL* (**b**, **d**). Grey arrowheads, putative TSSs. Representative of two biological replicates. **e**, Global analysis of host transcript cleavage by Cas13a. Cleavage ratio (black bar, mean) for every host transcript in the experiment shown in **c** ($P = 6.9 \times 10^{-64}$, $n = 1{,}027$ transcripts, unpaired two-sided Student's *t*-test). **f**, As in **e** but for the experiment shown in **d** ($P = 5.4 \times 10^{-32}$, $n = 1{,}092$ transcripts). **g**, As in **c** but for wild-type and ΔCRISPR *L. seeligeri* strains after addition of aTc to induce target transcription. **h**, As in **e** but for the experiment shown in **g** ($P = 6.9 \times 10^{-74}$, $n = 862$ transcripts).

that the function of the target transcript cleaved by the *cis*-RNase activity of Cas13a does not affect the potency of the type VI-A immune response. To determine the extent of Cas13a-mediated *trans*-RNA degradation in vivo, we used conventional RNA-seq (Extended Data Fig. 3a) as well as global mapping of RNA 5′ ends, a method that detects both the transcription start site (TSS) of primary transcripts and the products of Cas13a cleavage. We analysed both host- and phage-derived transcripts in the RR3, ΩCRISPR^{VI}(*spcE*) and ΩCRISPR^{VI}(*spcL*) strains of *L. ivanovii* after 105 min of infection with ϕRR4. In the absence of type VI-A immunity, we detected abundant peaks for each TSS over a background signal that is presumably derived from spurious RNA cleavage or alternative transcription initiation (Fig. 2a–d). By contrast, in ΩCRISPR^{VI}(*spcE*) cells we detected extensive cleavage within the ϕRR4 early lytic transcript (Fig. 2a) as well as within host transcripts (Fig. 2c, Extended Data Fig. 3b). Moreover, the average cleavage ratio (defined as the ratio of cleavage products to primary transcript reads) in ΩCRISPR^{VI}(*spcE*) cells was significantly ($P = 6.9 \times 10^{-64}$) higher than in RR3 control cells across all host transcripts (Fig. 2e, Supplementary Information 2). Transcripts of the late lytic operon were undetectable in ΩCRISPR^{VI}(*spcE*) cells (Fig. 2a, Extended Data Fig. 3a) probably because the products of phage early lytic genes are required for late gene transcription. Similar results were obtained for ΩCRISPR^{VI}(*spcL*) cells (Fig. 2b, d, f, Extended Data Fig. 3a, Supplementary Information 3). We also detected cleavage of the early lytic transcripts in this strain, presumably as a consequence of *trans*-RNA degradation by Cas13a. Finally, similar degradation of host RNA was observed in the absence of phage infection, 15 min after activation of Cas13a by a chromosomally encoded target in *L. seeligeri* ATCC35967 (Fig. 3g, h, Extended Data Fig. 3c, Supplementary Information 4). Together, these results indicate that *trans*-RNA cleavage by Cas13a leads to massive degradation of both host and invader RNA in vivo.

Whereas DNA-cleaving CRISPR–Cas systems provide immunity through direct destruction of the phage genome[7,15], we reasoned that the collateral RNA degradation deployed by type VI-A systems might lead to the depletion of host and phage factors that are required for phage DNA replication and thereby indirectly support the clearance of invader genomes. We used quantitative PCR (qPCR) to measure the abundance of phage DNA in the RR3 and ΩCRISPR^{VI} strains over the course of ϕRR4 infection (Fig. 3a). Phage DNA did not accumulate when early-expressed transcripts were targeted by *spcA* or *spcE*, probably because destruction of host and phage transcripts by Cas13a early in the lytic cycle prevented phage replication. By contrast, when Cas13a was programmed with *spcL*, phage DNA accumulated to similar levels to the RR3 control. This result indicates that Cas13a can interfere with phage infection at any time during the viral lytic cycle, through a mechanism that does not necessarily prevent the accumulation of phage DNA. We hypothesized that such a mechanism could be based on the growth defect observed during targeting of plasmids by Cas13 in both heterologous and native hosts[8,14]. We looked for similar growth defects during phage infection by measuring the OD_{600} of *L. ivanovii* RR3 and ΩCRISPR^{VI} cultures after infection. Although we detected only mild growth defects at a multiplicity of infection (MOI) of 1 (Extended Data Fig. 4a), at an MOI of 5, CRISPR targeting resulted in a marked growth delay of the cultures (Fig. 3b). It has been hypothesized that, similarly to abortive infection systems that elicit phage defence in other bacteria[17–19], massive host transcript degradation could result in dormancy of infected cells and thus prevent viral propagation[8,16]. To test this idea, we assessed cell viability and phage titres before and immediately after infection at an MOI of 2, as well as after the first phage burst 4 h later (Fig. 3c, Extended Data Fig. 4b). Only 10–20% of RR3 control cells lacking CRISPR remained viable immediately after infection, and these suffered a more pronounced loss after 4 h. By contrast, all three ΩCRISPR^{VI} strains exhibited the same initial loss of viability but then recovered at 4 h, although they showed reduced numbers compared to uninfected control cultures (Fig. 3c, Extended Data Fig. 4c). Phage titres mirrored these results, with substantial phage proliferation in RR3 cells during the first 4 h of infection, but a substantial decrease in phage propagation, even immediately after infection, in cells equipped with type VI-A immunity (Fig. 3d).

These results support a model for Cas13a-mediated immunity in which infected cells stop proliferating and inactivate the phages that invaded them, thus providing passive protection to uninfected cells, which survive and proliferate. Indeed, a viability of 10–20% corresponds to the expected number of uninfected cells at an MOI of 2, which calculated using the Poisson distribution is 13%. To test this model, we first tested whether Cas13a activation elicits cell dormancy. We monitored growth (OD_{600}) after induction of a P_{tet}-controlled target transcript by anhydrotetracycline (aTc) in the native type VI-A host, *L. seeligeri* ATCC35967 (Extended Data Fig. 5a). Wild-type (but not ΔCRISPR) cells exhibited growth arrest, with no evidence of lysis. These cultures recovered upon removal of aTc and remained sensitive to re-exposure to the inducer (Extended Data Fig. 5b), suggesting that the Cas13a-induced dormancy state is reversible. To test this more rigorously, we counted viable cells after induction of Cas13a targeting, plating culture samples on solid medium without aTc. Over the course of 9 h of target transcription and Cas13a activation, we observed a stable population of viable cells that could form colonies when aTc was removed (Fig. 3e), demonstrating that cells in which Cas13a was

activated cease to grow but do not die. Notably, these cells were not escape mutants that had lost CRISPR function; these accounted for only about 1% of the viable population after 9 h (Fig. 3e). Furthermore, induction of Cas13a in wild-type cells, but not in ΔCRISPR cells, provided tolerance to transient exposure to the bactericidal antibiotics ampicillin, ciprofloxacin and streptomycin, which are otherwise lethal to growing cells (Fig. 3f). Finally, to test whether cells enter a dormant state during phage targeting, we took samples of *L. ivanovii* RR3 and ΩCRISPR^{VI} cultures at different times after ϕRR4 infection to count viable cells and determine the vitality of the culture using the reagent resazurin, which is quantitatively converted to fluorescent resorufin by the reducing cytosol of living cells[20]. The colony-forming unit (CFU) values mimicked the results shown in Fig. 3c (Extended Data Fig. 5c). By contrast, resorufin fluorescence remained constant over the course of the experiment in ΩCRISPR^{VI} cultures (Extended Data Fig. 5d), showing that most cells in the culture, including those not able to form a colony, stayed alive during infection. Together, these data show that, when activated by a target transcript, the RNase activity of Cas13a promotes a state of cell dormancy, rather than cell death. Although dormancy can be reversed by the inhibition of target transcription, it is maintained in infected cells where active phages continue to produce protospacer RNA.

Next, we investigated whether infected cells could provide herd immunity to uninfected cells in the population, as has been observed for other CRISPR types[12,21,22]. We found that phage-sensitive, chloramphenicol-resistant RR3 cells were protected from ϕRR4 infection when co-cultured with ΩCRISPR^{VI}(*spcE*) cells (Fig. 3g). Finally, we directly tested whether the cell dormancy triggered by activation of Cas13a is sufficient to protect against phage infection. We introduced a plasmid harbouring a target under an aTc-inducible promoter into *L. ivanovii* ΩCRISPR^{VI}(*spcP*), which carries a spacer that matches the plasmid target, but not any of the phage transcripts. Pre-activation of Cas13a by aTc-induced target transcription resulted in a 6.7-fold reduction in ϕRR4 infection efficiency (Fig. 3h). Furthermore, the plasmid-targeting strain showed a significant ($P = 5 \times 10^{-4}$) survival advantage after 7 h of ϕRR4 infection (Extended Data Fig. 5e). Together, these results demonstrate that the *trans*-RNA degradation activity of Cas13a is sufficient to provide immunity against double-stranded DNA (dsDNA) phages by inducing dormancy in infected cells, which prevents viral proliferation and protects uninfected cells in the population.

Our observation that plasmid-activated type VI-A CRISPR immunity also protected against infection by a phage not recognized by the crRNA guide of Cas13a demonstrates that these systems can provide general, non-specific immunity. This suggests that type VI-A systems could neutralize 'escaper' phages in the population, which contain target mutations that prevent their recognition by the crRNA guide. Such escaper phages easily overcome DNA-targeting CRISPR systems[11–13] but should not be able to successfully infect a host in which a previous infection by a wild-type phage activated Cas13a (a very likely scenario when escapers are rare in the phage population). Indeed, we were not able to detect escaper plaques on lawns of *L. ivanovii* ΩCRISPR^{VI}(*spcE*) or ΩCRISPR^{VI}(*spcA*) cells (Extended Data Fig. 6a, b). To investigate the ability of type VI-A systems to protect against escaper phages, we engineered two ϕRR4 mutants that could escape *spcA* (ϕRR4^{acr}) and *spcE* (ϕRR4^{early}) targeting (Extended Data Figs. 6a-d). We infected *L. ivanovii* ΩCRISPR^{VI} cells with these mutants and found that escaper phage propagation was reduced by 1–2 orders of magnitude when cells were co-infected (1:10^5 ratio) with wild-type ϕRR4 (Fig. 4a, c). Moreover, we obtained similar results when we used the virulent myovirus A511[23], a *Listeria* phage unrelated to ϕRR4, instead of the mutants (Fig. 4b, c). Finally, we tested the prediction that the extent of escaper neutralization should increase with the MOI, as the probability of infection with a wild-type phage also increases. Indeed, cells pre-infected at higher MOIs with wild-type ϕRR4 showed reduced propagation of escaper phages (added at MOI 0.1 to pre-infected cells) (Fig. 4d). Adsorption efficiency was unchanged after the first infection, excluding the possibility that competition for phage binding sites prevented the second

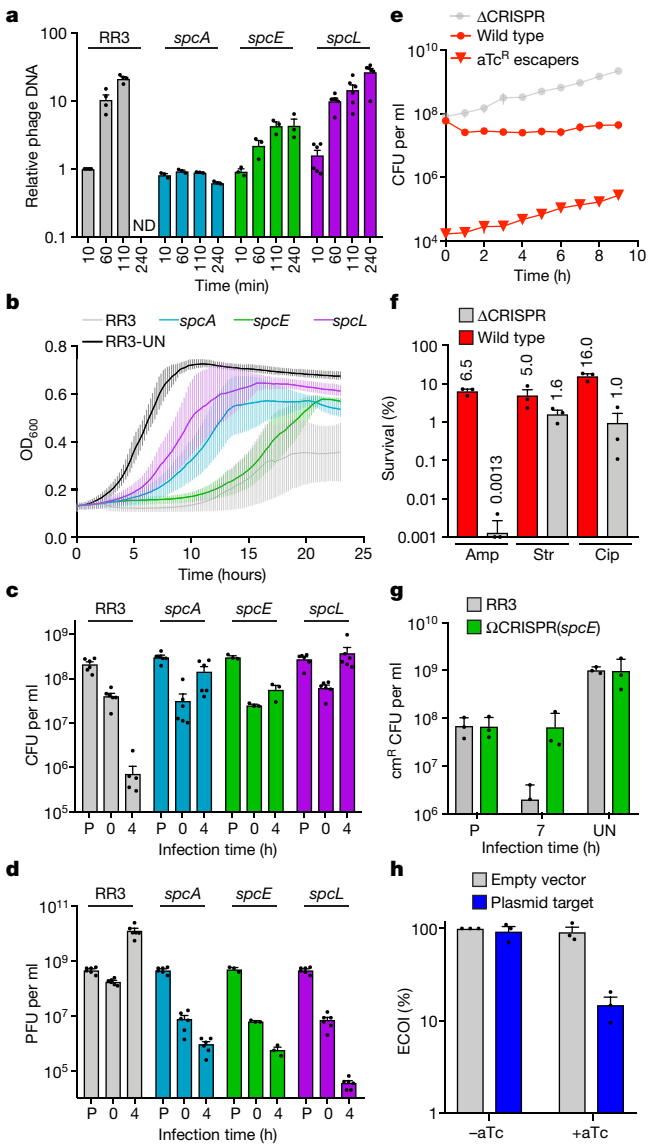

Fig. 3 | Cas13a-induced cell dormancy is sufficient to abort lytic infection and limit phage propagation. a, Mean (± s.e.m., $n = 3$ biological replicates) phage DNA content after infection of *L. ivanovii* RR3 and ΩCRISPR^{VI}(*spcA*, *spcE* or *spcL*) strains with ϕRR4 at an MOI of 1, normalized to value for RR3 cells 10 min after infection. **b**, Mean (± s.e.m., $n = 3$ biological replicates) OD_{600} values of *L. ivanovii* RR3 and ΩCRISPR^{VI}(*spcA*, *spcE* or *spcL*) cultures after infection with ϕRR4 at an MOI of 5. RR3-UN, uninfected RR3. **c**, Mean (± s.e.m., $n = 6$ biological replicates) CFU present in *L. ivanovii* RR3 and ΩCRISPR^{VI}(*spcA*, *spcE* or *spcL*) cultures before (P), immediately after (0), and 4 h after infection with ϕRR4 at an MOI of 2. **d**, As in **c** but measuring PFU titre. **e**, Mean (± s.e.m., $n = 3$ biological replicates) CFU from *L. seeligeri* wild-type and ΔCRISPR cultures after transcription of a chromosomal target and plating on medium lacking aTc. Escaper mutants in the wild-type culture were counted on plates with aTc. **f**, Mean (± s.e.m., $n = 3$ biological replicates) survival of *L. seeligeri* wild-type and ΔCRISPR cultures in the presence of ampicillin (Amp), streptomycin (Str) or ciprofloxacin (Cip) after activation of Cas13. **g**, Mean (± s.e.m., $n = 3$ biological replicates) chloramphenicol-resistant CFU per ml before (P), 7 h after (7) and without (UN) infection with ϕRR4 at an MOI of 1 of a 1:1 mix of phage-susceptible, chloramphenicol-resistant (cm^R) *L. ivanovii* RR3 and chloramphenicol-sensitive *L. ivanovii* RR3 or ΩCRISPR^{VI}(*spcE*) strains. **h**, Mean (± s.e.m., $n = 3$ biological replicates) ECOI after addition of ϕRR4 to phage-susceptible *L. ivanovii* ΩCRISPR^{VI}(*spcP*) cells harbouring a plasmid with an aTc-inducible *spcP* target or an empty vector control.

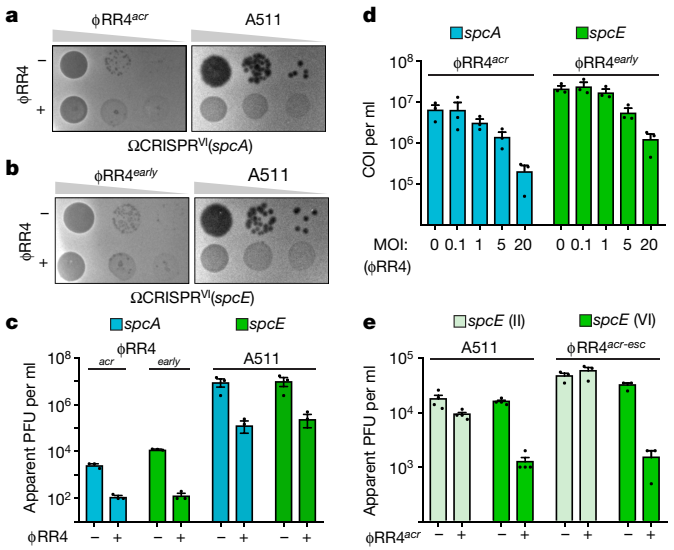

Fig. 4 | Activation of Cas13a suppresses viral escape by providing immunity against untargeted phage. a, ϕRR4^{acr} (*spcA*-escaper) or A511 was diluted in the presence or absence of 10^5-fold excess wild-type ϕRR4, and plated on *L. ivanovii* ΩCRISPR^{VI}(*spcA*) lawns. Examples are representative of three biological replicates. **b**, As in **a**, but using a ΩCRISPR^{VI}(*spcE*) strain and the *spcE*-escaper ϕRR4^{early}. **c**, Mean (± s.e.m., $n = 3$ biological replicates) PFU titres obtained in **a**, **b**. **d**, Mean (± s.e.m., $n = 3$ biological replicates) centre of infection (COI) titre of ϕRR4^{acr} and ϕRR4^{early} escaper phages after infection at an MOI of 0.1 of ΩCRISPR^{VI}(*spcA*) and ΩCRISPR^{VI}(*spcE*) cells, respectively, that were pre-infected for 2 h with wild-type ϕRR4 at the indicated MOIs. **e**, Mean (± s.e.m., $n = 3$ biological replicates) plaque-forming efficiency for A511 and ϕRR4$^{acr\text{-}esc}$ (a Cas9 escape mutant derived from ϕRR4^{acr}) phages on ΩCRISPR^{II}(*spcE*) or ΩCRISPR^{VI}(*spcE*) cells, in the presence and absence of excess ϕRR4^{acr}.

infection by escaper phages (Extended Data Fig. 6e). As a control, we infected a ΩCRISPR^{II}(*spcE*) strain that carried the type II-A CRISPR system from *Streptococcus pyogenes* programmed with *spcE* with ϕRR4^{acr}, which lacks the anti-CRISPR genes that inhibit Cas9 cleavage (Extended Data Fig. 6c, f). We isolated one Cas9-resistant escaper phage (ϕRR4$^{acr\text{-}esc}$) and used it to co-infect either ΩCRISPR^{II}(*spcE*) or ΩCRISPR^{VI}(*spcE*) cells with 10^5-fold excess ϕRR4^{acr} (Fig. 4e). While Cas13a activation with ϕRR4^{acr} provided protection against ϕRR4$^{acr\text{-}esc}$ (and similarly, A511), co-infection with ϕRR4^{acr} did not prevent either ϕRR4$^{acr\text{-}esc}$ or A511 from escaping Cas9 targeting. Therefore, cross-protection is a feature of Cas13a targeting, and not a ϕRR4-specific phenomenon, such as superinfection exclusion. Together, these data indicate that type VI-A immunity against wild-type ϕRR4 cross-protects against infection by both protospacer escape mutant phages and other unrelated viruses. Thus, by acting on the infected host rather than directly on the target phage, Cas13a activation leads to broad and nonspecific immunity against dsDNA phages.

We have shown that during the type VI-A CRISPR–Cas response against dsDNA phages, the RNase Cas13a performs crRNA-guided recognition of phage RNA, resulting in massive degradation of host and phage transcripts. Although it is possible that this degradation interferes with the phage lytic cycle to contribute to overall defence, we believe that the fundamental feature of type VI-A immunity is the dormancy of the host cell produced by the destruction of host transcripts. This is similar to other phage defence strategies known as abortive infection[24]. We postulate that, in the absence of a mechanism to specifically destroy the phage DNA, target transcription continues, Cas13a remains active and the host cells neither resume growth nor lyse. Therefore, the infected cell can continue to adsorb phages, abort their infectious cycle and eliminate them from the culture.

To our knowledge, all other CRISPR types studied possess DNA cleavage activities that can destroy the genome of an infecting phage[6,7,15,25,26]. Therefore immunity is achieved by a direct attack on the invader, followed by survival of the infected cells. A consequence of direct interference with the phage lytic cycle is that mutant escapers can overcome targeting, kill the infected cell and propagate. By contrast, during type VI-A CRISPR–Cas immunity, the small fraction of escaper phages present in the viral population are likely to end up infecting a cell in which Cas13a was previously activated by a wild-type, target-bearing phage, and are therefore also neutralized. Phage density, escaper frequency, and spacer targeting efficiency are all likely to affect the extent of this cross-protection mechanism.

Instead of using abortive infection to limit the propagation of escaper phages, the DNA-degrading CRISPR systems usually acquire new spacer sequences that can target other regions of the phage[12]. Given the negative selection suffered by cells in which type VI-A immunity is triggered, and the strong protection against escapers provided by Cas13a, it is unclear how spacer acquisition might operate in these systems. One possibility is that spacers are acquired from the injected genomes of defective phage particles that fail to activate their transcriptional program[27]. Alternatively, phage genomes could occasionally be cleared from the cell after Cas13a activation, permitting the cell to recover from dormancy. If such a mechanism exists, the infected cell itself would benefit from the presence of the type VI CRISPR system and immunity would not be an exclusively altruistic event.

Online content

Any methods, additional references, Nature Research reporting summaries, source data, extended data, supplementary information, acknowledgements, peer review information; details of author contributions and competing interests; and statements of data and code availability are available at https://doi.org/10.1038/s41586-019-1257-5.

Received: 8 January 2019; Accepted: 30 April 2019;
Published online: 29 May 2019

1. Mojica, F. J., Díez-Villaseñor, C., García-Martínez, J. & Soria, E. Intervening sequences of regularly spaced prokaryotic repeats derive from foreign genetic elements. *J. Mol. Evol.* **60**, 174–182 (2005).
2. Bolotin, A., Quinquis, B., Sorokin, A. & Ehrlich, S. D. Clustered regularly interspaced short palindrome repeats (CRISPRs) have spacers of extrachromosomal origin. *Microbiology* **151**, 2551–2561 (2005).
3. Pourcel, C., Salvignol, G. & Vergnaud, G. CRISPR elements in *Yersinia pestis* acquire new repeats by preferential uptake of bacteriophage DNA, and provide additional tools for evolutionary studies. *Microbiology* **151**, 653–663 (2005).
4. Barrangou, R. et al. CRISPR provides acquired resistance against viruses in prokaryotes. *Science* **315**, 1709–1712 (2007).
5. Brouns, S. J. et al. Small CRISPR RNAs guide antiviral defense in prokaryotes. *Science* **321**, 960–964 (2008).
6. Marraffini, L. A. & Sontheimer, E. J. CRISPR interference limits horizontal gene transfer in staphylococci by targeting DNA. *Science* **322**, 1843–1845 (2008).
7. Garneau, J. E. et al. The CRISPR/Cas bacterial immune system cleaves bacteriophage and plasmid DNA. *Nature* **468**, 67–71 (2010).
8. Abudayyeh, O. O. et al. C2c2 is a single-component programmable RNA-guided RNA-targeting CRISPR effector. *Science* **353**, aaf5573 (2016).
9. Smargon, A. A. et al. Cas13b is a type VI-B CRISPR-associated RNA-guided RNase differentially regulated by accessory proteins Csx27 and Csx28. *Mol. Cell* **65**, 618–630.e617 (2017).
10. Yan, W. X. et al. Cas13d is a compact RNA-targeting type VI CRISPR effector positively modulated by a WYL-domain-containing accessory protein. *Mol. Cell* **70**, 327–339.e325 (2018).
11. Deveau, H. et al. Phage response to CRISPR-encoded resistance in *Streptococcus thermophilus*. *J. Bacteriol.* **190**, 1390–1400 (2008).
12. van Houte, S. et al. The diversity-generating benefits of a prokaryotic adaptive immune system. *Nature* **532**, 385–388 (2016).
13. Pyenson, N. C., Gayvert, K., Varble, A., Elemento, O. & Marraffini, L. A. Broad targeting specificity during bacterial type III CRISPR–Cas immunity constrains viral escape. *Cell Host Microbe* **22**, 343–353.e343 (2017).
14. Meeske, A. J. & Marraffini, L. A. RNA guide complementarity prevents self-targeting in type VI CRISPR systems. *Mol. Cell* **71**, 791–801.e793 (2018).
15. Westra, E. R. et al. CRISPR immunity relies on the consecutive binding and degradation of negatively supercoiled invader DNA by Cascade and Cas3. *Mol. Cell* **46**, 595–605 (2012).
16. Koonin, E. V. & Zhang, F. Coupling immunity and programmed cell suicide in prokaryotes: life-or-death choices. *BioEssays* **39**, 1–9 (2017).
17. Parreira, R., Ehrlich, S. D. & Chopin, M. C. Dramatic decay of phage transcripts in lactococcal cells carrying the abortive infection determinant *AbiB*. *Mol. Microbiol.* **19**, 221–230 (1996).
18. Fineran, P. C. et al. The phage abortive infection system, ToxIN, functions as a protein-RNA toxin-antitoxin pair. *Proc. Natl Acad. Sci. USA* **106**, 894–899 (2009).

19. Short, F. L. et al. Selectivity and self-assembly in the control of a bacterial toxin by an antitoxic noncoding RNA pseudoknot. *Proc. Natl Acad. Sci. USA* **110**, E241–E249 (2013).
20. Shiloh, M. U., Ruan, J. & Nathan, C. Evaluation of bacterial survival and phagocyte function with a fluorescence-based microplate assay. *Infect. Immun.* **65**, 3193–3198 (1997).
21. Watson, B. N. J., Staals, R. H. J. & Fineran, P. C. CRISPR–Cas-mediated phage resistance enhances horizontal gene transfer by transduction. *MBio* **9**, e02406-17 (2018).
22. Payne, P., Geyrhofer, L., Barton, N. H. & Bollback, J. P. CRISPR-based herd immunity can limit phage epidemics in bacterial populations. *eLife* **7**, e32035 (2018).
23. Klumpp, J. et al. The terminally redundant, nonpermuted genome of *Listeria* bacteriophage A511: a model for the SPO1-like myoviruses of gram-positive bacteria. *J. Bacteriol.* **190**, 5753–5765 (2008).
24. Rostøl, J. T. & Marraffini, L. (Ph)ighting phages: how bacteria resist their parasites. *Cell Host Microbe* **25**, 184–194 (2019).
25. Yan, W. X. et al. Functionally diverse type V CRISPR–Cas systems. *Science* **363**, 88–91 (2019).
26. Zetsche, B. et al. Cpf1 is a single RNA-guided endonuclease of a class 2 CRISPR–Cas system. *Cell* **163**, 759–771 (2015).
27. Hynes, A. P., Villion, M. & Moineau, S. Adaptation in bacterial CRISPR–Cas immunity can be driven by defective phages. *Nat. Commun.* **5**, 4399 (2014).

METHODS

No statistical methods were used to predetermine sample size. The experiments were not randomized and the investigators were not blinded to allocation during experiments and outcome assessment.

Bacterial strains and growth conditions. The type VI CRISPR system was derived from *L. seeligeri* ATCC strain 35967 (Rocourt and Grimont). *L. seeligeri* RR4 and *L. ivanovii* RR3 were obtained from J.-P. Lemaître (INRA, Dijon, France). All *Listeria* strains were propagated in Brain Heart Infusion (BHI) broth or agar at 30 °C. Unless otherwise stated, plasmids were cloned in *Escherichia coli* DH5α, miniprepped, and transformed into the conjugative donor strain *E. coli* SM10 for conjugative mating. All *E. coli* strains were cultured in lysogeny broth (LB) at 37 °C.

Phage isolation and propagation. Isolation of ϕRR4 was carried out by overnight induction of *L. seeligeri* RR4 at OD 0.1 using mitomycin C at 2 μg/ml. The induced culture supernatant was diluted to single plaques on a lawn of *L. ivanovii*, and a single plaque was purified twice to ensure homogeneity. To generate high-titre phage lysates, 50 ml of *L. ivanovii* culture was infected with ϕRR4 at MOI 0.1, OD 0.1 and the infection proceeded overnight. The lysate was filtered and concentrated to 1 ml using Amicon Ultra 100MWCO columns.

Infective centre and burst size quantification. *L. ivanovii* strains were grown to mid-exponential phase, and 0.6 ml of culture at OD_{600} 0.5 was infected with ϕRR4 or derivatives at an MOI of 0.1. Adsorption was carried out for 5 min, followed by three washes with 1 ml BHI to remove unbound phage, and the samples were resuspended to a final volume of 1 ml. Infective centres were enumerated by measuring PFU titres on a lawn of naive *L. ivanovii* RR3 at the initial time point. Burst size was calculated by dividing the PFU after the first burst by the starting PFU.

***E. coli–Listeria* conjugation.** Donor *E. coli* SM10 or β2163 Δ*dapA* strains carrying *E. coli–Listeria* shuttle vectors were cultured in LB containing 100 μg/ml ampicillin (for pAM8-derived vectors) or 25 μg/ml chloramphenicol (for pPL2e-derived vectors). Recipient *L. seeligeri* or *L. ivanovii* strains were cultured in BHI. Saturated donor and recipient cultures (100 μl each) were combined in 10 ml BHI, and concentrated onto a 0.45-μm membrane filter, which was then overlaid onto a BHI agar plate containing 8 μg/ml oxacillin, which weakens the cell wall, enhancing conjugation. Mating plates were incubated for 4 h at 37 °C, then cells were resuspended in 2 ml BHI and plated at 30 °C on selective BHI medium containing 50 μg/ml nalidixic acid (which kills donor *E. coli* but not recipient *Listeria*). Selection for plasmid recipients was performed with either 15 μg/ml chloramphenicol (for pAM8-derived vectors) or 1 μg/ml erythromycin (for pPL2e-derived vectors).

Cloning of CRISPR locus and spacer library construction. The *L. seeligeri* type VI CRISPR locus was introduced into *L. ivanovii* RR3 by cloning into the PSA site-specific integrating vector pPL2e[28] via three-piece Gibson assembly using (1) a synthetic gene fragment containing the native promoter and CRISPR array modified to contain only two repeats and BsaI sites for spacer cloning (amplified with oAM462/127), (2) the *cas13a* gene (amplified with oAM463/94), and (3) BamHI-SalI-digested pPL2e, resulting in the plasmid pAM125. Cloning of individual spacers was carried out by ligation of annealed oligos into BsaI-digested pAM125. For spacer library construction, a library of 41,276 × 85-nt oligonucleotides, each containing a unique ϕRR4-matching spacer, repeat homology, BsaI sites, and universal priming sites, was purchased from Twist Biosciences. The library was made double-stranded by PCR and the product was purified by phenol-chloroform extraction. Spacers were introduced into pAM125 via Golden Gate cloning with BsaI-HFv2 (New England Biolabs) and T7 DNA ligase, then electroporated into Endura Duo electrocompetent cells. Four hundred thousand colonies were pooled, and the plasmids were isolated and electroporated into the conjugative donor strain β2163 Δ*dapA* in the presence of 1.2 mM diaminopimelic acid (DAP). Conjugation into *L. ivanovii* was carried out as described above, except for the presence of 1.2 mM DAP during mating. Transconjugants were isolated in the presence of erythromycin (to select for ΩCRISPR^{VI} integration) and the absence of DAP to prevent growth of the auxotrophic donor *E. coli*. The ΩCRISPR^{II} strain was constructed by cloning the type II-A CRISPR–Cas9 system from *S. pyogenes* into the *E. coli–Listeria* shuttle vector pAM8[14]. A single spacer was retained with two SapI sites for spacer cloning (pAM307). Cloning of individual spacers was carried out by ligation of annealed oligos into SapI-digested pAM307. A pAM307 variant carrying ϕRR4 *spcE* (pAM325) was conjugated into *L. ivanovii*, selecting on medium containing 50 μg/ml nalidixic acid and 15 μg/ml chloramphenicol to generate ΩCRISPR^{II}.

Gene deletions and replacements in *Listeria*. Allelic replacement in *L. seeligeri* or *L. ivanovii* was conducted as previously described[14]. In brief, 1-kb homologous sequences flanking each side of the region to be replaced were cloned into pAM215, a suicide plasmid unable to replicate in *Listeria*, that also carries *lacZ* and chloramphenicol resistance (*cat*) markers. This plasmid was transferred to *Listeria* strains via conjugation as described above, and 100 μl of resuspended cells was plated for selection on 50 μg/ml nalidixic acid and 15 μg/ml chloramphenicol. Isolated transconjugants (integrants) were streak-purified and confirmed *lacZ*+ by patching on BHI plates containing 100 μg/ml 5-bromo-4-chloro-3-indolyl β-D-galactopyranoside (X-gal). Integrants were passaged (grown to saturation, then diluted 1,000-fold) 3–4 times in BHI without selection. Passaged cultures were diluted and plated on BHI X-gal, and incubated for 2–3 days at 37 °C. White (*lacZ*$^-$) colonies (excisants) were isolated, confirmed chloramphenicol-sensitive, and checked for the deletion by PCR using primers flanking the desired deletion followed by Sanger sequencing.

Bacterial genome sequencing and assembly. Chromosomal DNA was prepared from 2-ml cultures of *L. seeligeri* RR4 and *L. ivanovii* RR3 via lysozyme treatment and phenol-chloroform extraction and ethanol precipitation. DNA samples were sheared using a Covaris sonicator and prepared for deep sequencing using the Illumina TruSeq Nano DNA LT kit, and paired-end 2 × 300-bp sequencing was conducted on the MiSeq platform. Reads were quality-trimmed using Sickle (https://github.com/najoshi/sickle), and assembled into contigs using Abyss (https://github.com/bcgsc/abyss). Finally, contigs were mapped to reference *L. seeligeri* and *L. ivanovii* genomes using Medusa (http://combo.dbe.unifi.it/medusa). Automated genome annotation was performed using BaSys (https://www.basys.ca). Raw reads and assembled genomes have been deposited to GenBank under BioProject accession number PRJNA512236.

Spacer selection, deep sequencing and analysis. The spacer library was grown to OD 0.3 and a pre-infection sample was harvested. The remaining culture was infected with ϕRR4 at an MOI of 1, and surviving cells were harvested 5 h later. Chromosomal DNA was prepared from both samples, and the CRISPR array was amplified using oAM459/16. Library preparation from the resulting PCR products was conducted using the Illumina TruSeq Nano DNA LT kit, followed by 150-bp single-end sequencing using the MiSeq platform. Spacer sequences flanked by perfect repeats were extracted and mapped to the ϕRR4 genome using bowtie2. Reads at each position in the genome were calculated and normalized to total spacer reads, and the enrichment ratio for a given spacer was calculated as the post-infection read count divided by the pre-infection read count. Spacers with fewer than 10 reads before infection were discarded to reduce noise (26,766 spacers retained). Raw sequencing reads for each time point have been deposited under BioProject accession number PRJNA512236.

RNA sequencing. To isolate RNA from *Listeria*, the equivalent of 3 ml culture at OD_{600} 0.5 was pelleted and lysed by 3 min treatment with 2 mg/ml lysozyme followed by the addition of sarkosyl at 1%. A fixed amount of *Staphylococcus aureus* RNA was added to each sample immediately after lysis for global RNA normalization. RNA was purified from these lysates using the Zymo Direct-Zol RNA miniprep plus kit according to the manufacturer's instructions. Genomic DNA was eliminated using the Ambion Turbo DNase-free kit. Ribosomal RNA was depleted using the Illumina Ribo-Zero rRNA removal (Bacteria) kit. After rRNA removal, libraries were prepared for deep sequencing using the TruSeq Stranded mRNA Library prep kit, skipping mRNA purification and beginning at the RNA fragmentation step. Paired-end (2 × 75-bp) sequencing was performed on the NextSeq platform. Paired-end sequencing data for phage-infected *L. ivanovii* RR3, ΩCRISPR^{VI}(*spcE*), and ΩCRISPR^{VI}(*spcL*) strains, as well as aTc-treated *L. seeligeri* wild-type (Ptet-*spc4*) and ΔCRISPR (Ptet-*spc4*) strains, have been deposited under BioProject accession number PRJNA512236.

For 5′ end mapping, RNA was first purified, DNase-treated and rRNA depleted as above, then concentrated using the Zymo RNA Clean & Concentrator 5 kit and 5′ phosphorylated with T4 polynucleotide kinase (NEB). 5′ triphosphates were removed using *E. coli* polyphosphatase, and a 5′ RNA adaptor was added using T4 RNA ligase. The library was fragmented using Agilent RNA fragmentation reagents, and reverse transcribed using SuperScript IV with an adaptor primer ending in nine randomized nucleotides. The resulting cDNA libraries were amplified by PCR and purified using AMPure beads, then single-end 150-bp sequencing was carried out on the MiSeq platform. 5′ end sequencing data for phage-infected *L. ivanovii* RR3, ΩCRISPR^{VI}(*spcE*), and ΩCRISPR^{VI}(*spcL*) strains, as well as aTc-treated *L. seeligeri* wild-type (Ptet-*spc4*) and ΔCRISPR (Ptet-*spc4*) strains, have been deposited under BioProject accession number PRJNA512236.

RNA-seq analysis. RNA-seq reads were mapped to the corresponding genome using bowtie2. Coverage was calculated at each genome position and normalized to the total number of *S. aureus* reads (representing the spike-in), and the ratio of CRISPR$^+$:CRISPR$^-$ reads was calculated. If zero reads were detected, a pseudocount was added. For RNA 5′ end mapping analysis, reads were mapped as above, with only the 5′ end position tabulated. Operonic transcripts were manually annotated from the paired-end transcriptomic data, and these boundaries were used to calculate the fraction of reads that mapped within or outside the TSS. The site within 500 nucleotides upstream of the start codon containing the most 5′ reads in wild-type cells was designated as the TSS. Reads mapping within five nucleotides of this site were counted as TSS reads. For transcripts in which at least 20 reads were detected in each sample, the cleavage ratio was calculated as the read count downstream of the TSS divided by that within the TSS. Normalization to the TSS accounts for differences in gene expression generated by pleiotropic effects such as the degradation of transcription factor mRNAs. This cleavage

ratio also allowed us to capture events in which Cas13a-mediated degradation did not produce stable cleavage products. Tables are provided showing cleavage ratios for each transcript in phage-infected *L. ivanovii* RR3 and ΩCRISPR^{VI}(*spcE*) (Supplementary Information 2), ΩCRISPR^{VI}(*spcL*) (Supplementary Information 3), and aTc-treated *L. seeligeri* wild-type (Ptet-*spc4*) and ΔCRISPR (Ptet-*spc4*) (Supplementary Information 4) strains.

ϕRR4 escaper mutant construction. ϕRR4 mutants were generated by allelic exchange using the integration of the suicide vector pAM215 into the *L. seeligeri* RR4 lysogen as described above. Mutant prophages were confirmed by PCR and sequencing, and induced with mitomycin C as described above.

Herd immunity experiment. *L. ivanovii* RR3 cells carrying a *cat* gene encoding resistance to chloramphenicol were co-cultured at a 1:1 ratio with either wild-type RR3 or ΩCRISPR^{VI}(*spcE*) cells, then the population was infected with ϕRR4 at $OD_{600} = 0.1$, MOI 1, for 7 h at 30 °C. Viable chloramphenicol-resistant cells were counted before and 7 h after infection.

Immunity by plasmid targeting. *L. ivanovii* ΩCRISPR^{VI}(*spcP*) cells were transformed with pAM211 (empty vector) or pAM212 (aTc-inducible *spcP* target) via conjugative mating. Cells carrying each plasmid and the CRISPR locus were grown to $OD_{600} = 0.1$, and exposed to 100 ng/ml aTc for 1h. Then, cells were infected with ϕRR4 at MOI 1 for 7 h at 30 °C. Viable CFUs were counted before and after infection. Alternatively, the efficiency of ϕRR4 infective centre formation was measured on cells 1 h after aTc treatment.

Cell vitality assay. Cell vitality was measured with the resazurin-based cell vitality reagent alamarBlue HS (ThermoFisher) according to the manufacturer's instructions. In brief, 100 μl of cell culture was mixed with 10 μl of alamarBlue HS and incubated for 20 min while shaking at 37 °C, and fluorescence (excitation: 560 nm, emission: 590 nm) was measured on a Tecan Infinite M200 Pro plate reader with monochromator module with a fixed gain setting of 79. Uninfected cells in the same medium as all experimental samples were used as live cell standards, and the same samples heated for 5 min at 95 °C were used as dead cell standards. We made 10% and 50% live cell mixture standards to assess the accuracy of vitality measurements. Dead cell signal was subtracted as background from all resorufin signal values. Resorufin signal values for all samples were normalized to values before infection.

Phage co-infection plaque assays. For phage co-infection assays to assess the efficiency of escaper infection in the presence and absence of co-infecting wild-type phage, escaper phage stocks were diluted to approximately 5×10^4 PFU/ml in BHI medium, then mixed with BHI containing either no phage or 5×10^9 PFU/ml wild-type ϕRR4. Serial tenfold dilutions of phage mixtures were made and 2 μl of each dilution was spotted onto BHI top agar lawns seeded with 100 μl of saturated cultures of ΩCRISPR^{VI} strains. ϕRR4^{acr} escaper mixtures were spotted onto ΩCRISPR^{VI}(*spcA*) lawns, and ϕRR4^{early} escaper mixtures were spotted on ΩCRISPR^{VI}(*spcE*) lawns. A511 mixtures were spotted onto both targeting lawns. Co-infections comparing Cas9 and Cas13 were conducted in the same way, except that ϕRR4^{acr} was used as the activating phage, and was mixed in 10^5-fold excess with ϕRR4$^{acr\text{-}esc}$ or A511. Mixtures were spotted onto BHI top agar lawns seeded with 100 μl of saturated ΩCRISPR^{VI}(*spcE*) or ΩCRISPR^{II}(*spcE*) culture.

Reporting summary. Further information on research design is available in the Nature Research Reporting Summary linked to this paper.

Data availability

The *L. seeligeri* RR4 and *L. ivanovii* RR3 genome sequences, along with raw reads from the spacer library deep sequencing, paired-end RNA-seq, and 5′ end mapping have been deposited in the Sequence Read Archive under BioProject accession number PRJNA512236. Lists of strains, plasmids, and oligonucleotides used in this study are available in Supplementary Information 5.

Code availability

Custom scripts used in analysis of spacer library data as well as RNA 5′ end mapping data are available upon request.

28. Lauer, P., Chow, M. Y., Loessner, M. J., Portnoy, D. A. & Calendar, R. Construction, characterization, and use of two *Listeria monocytogenes* site-specific phage integration vectors. *J. Bacteriol.* **184**, 4177–4186 (2002).
29. Rocourt, J., Schrettenbrunner, A., Hof, H. & Espaze, E. P. [New species of the genus *Listeria*: *Listeria seeligeri*]. *Pathol. Biol. (Paris)* **35**, 1075–1080 (1987).
30. Lemaître, J. P., Duroux, A., Pimpie, R., Duez, J. M. & Milat, M. L. *Listeria* phage and phage tail induction triggered by components of bacterial growth media (phosphate, LiCl, nalidixic acid, and acriflavine). *Appl. Environ. Microbiol.* **81**, 2117–2124 (2015).
31. Loessner, M. J., Inman, R. B., Lauer, P. & Calendar, R. Complete nucleotide sequence, molecular analysis and genome structure of bacteriophage A118 of *Listeria monocytogenes*: implications for phage evolution. *Mol. Microbiol.* **35**, 324–340 (2000).

Acknowledgements We thank all members of the Marraffini laboratory for advice and encouragement, A. Varble for discussions, and J. T. Rostøl for critical reading of the manuscript. *L. seeligeri* RR4 and *L. ivanovii* RR3 were gifts from J.-P. Lemaître. Support for this work comes from the National Institute of Health Director's Pioneer Award 1DP1GM128184-01 (to L.A.M.). L.A.M. is an investigator of the Howard Hughes Medical Institute. A.J.M. is a Helen Hay Whitney postdoctoral fellow.

Author contributions Experiments were designed by A.J.M. and L.A.M. A.J.M. conducted spacer library construction and testing, all RNA sequencing, cell dormancy experiments, phage mutant construction, and escaper cross-protection assays, as well analysis of all next-generation sequencing data. S.N.-H. assisted with sequencing the *L. seeligeri* RR4 and *L. ivanovii* RR3 genomes and initial testing of spacers in ϕRR4 immunity. The paper was written by A.J.M. and L.A.M.

Competing interests L.A.M. is a cofounder and Scientific Advisory Board member of Intellia Therapeutics, and a co-founder of Eligo Biosciences. The other authors declare no competing interests.

Additional information

Supplementary information is available for this paper at https://doi.org/10.1038/s41586-019-1257-5.

Correspondence and requests for materials should be addressed to A.J.M. or L.A.M.

Peer review information *Nature* thanks Peter Fineran, Edze Westra and the other anonymous reviewer(s) for their contribution to the peer review of this work.

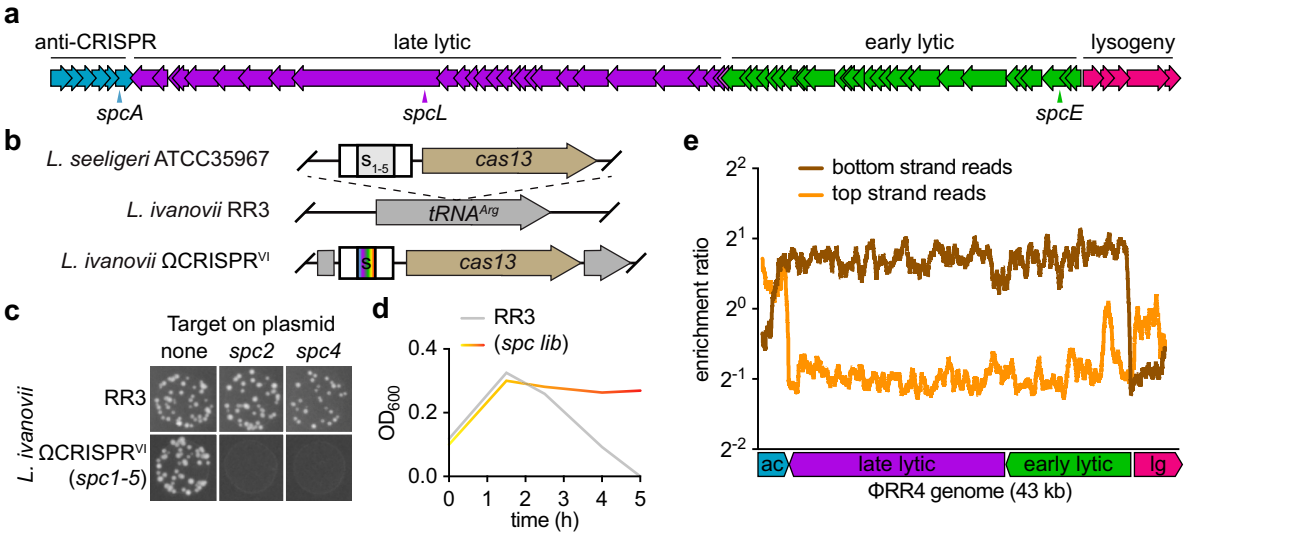

Extended Data Fig. 1 | *Listeria* phage infection model for studying type VI-A CRISPR immunity. a, Diagram of the ϕRR4 genome, with individual genes depicted within the anti-CRISPR, early lytic, late lytic, and lysogenic regions. *L. seeligeri* ATCC35967 harbours a five-spacer type VI-A CRISPR locus[29], but phages that infect this strain have not yet been identified. We sequenced the genome of *L. seeligeri* RR4[30] and found that it contains a 42-kb prophage, ϕRR4, that is similar to the A118 listeriophage[31]. Although ϕRR4 particles induced from the lysogen did not infect *L. seeligeri* ATCC35967, ϕRR4 propagated in the closely related *L. ivanovii* RR3 strain (99.2% 16S rRNA identity)[30]. **b**, The type VI-A CRISPR locus of *L. seeligeri* ATCC35967 was inserted into the *tRNA*^{Arg} gene of *L. ivanovii* RR3 using the vector pAM125, generating *L. ivanovii* ΩCRISPR^{VI}. Different strains with either the five spacers naturally present in this system (*spc1–5*), individual spacers matching the genome of ϕRR4 (*spcA*, *spcE*, *spcL*), or a ϕRR4 spacer library (*spc lib*), were generated. For the latter, 41,276 ϕRR4-matching spacers were selected, tiled every two nucleotides across the phage genome, with both strands equally represented. **c**, Test of type VI-A anti-plasmid immunity in *L. ivanovii* ΩCRISPR^{VI}(*spc1–5*). Plasmids with *spc2* or *spc4* targets in the chloramphenicol resistance cassette were conjugated into *L. ivanovii* RR3 or ΩCRISPR^{VI}(*spc1–5*) and transconjugants selected on nalidixic acid and chloramphenicol. Transconjugants that received an empty vector lacking a target sequence are shown as a negative control (none). Representative of two biological replicates. **d**, Prevention of ϕRR4 lytic infection by the type VI spacer library. Spacer library cells (yellow–orange gradient) or cells lacking CRISPR (grey) were infected with ϕRR4 at $OD_{600} = 0.1$, MOI = 1, and OD_{600} was monitored over time. Representative of two biological replicates. **e**, One-hundred-base-pair sliding window average spacer enrichment ratio (post-infection/pre-infection spacer abundance) for spacers targeting the top (orange) and bottom (brown) strands.

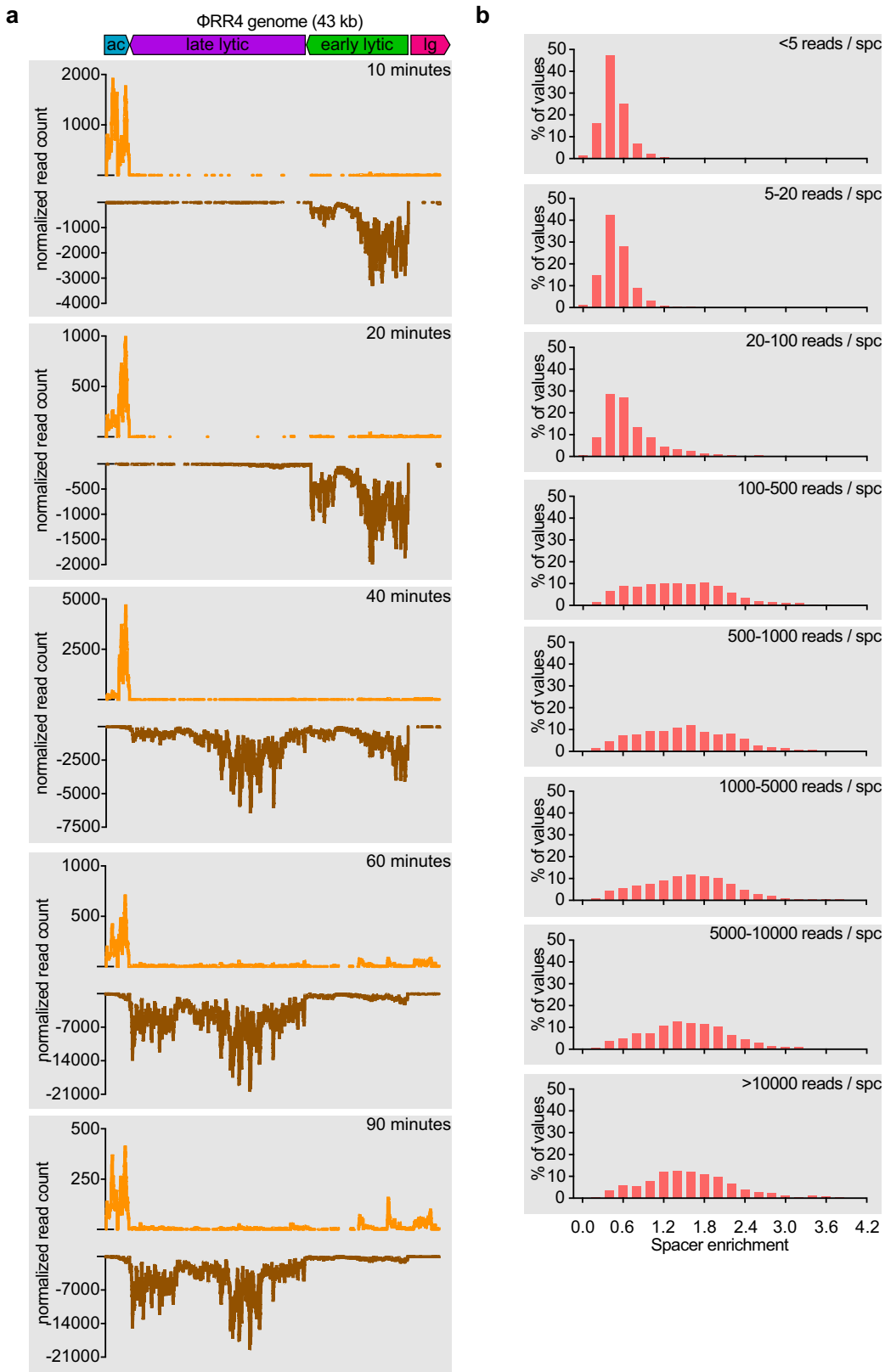

Extended Data Fig. 2 | ϕRR4 transcriptome and enrichment of corresponding targeting spacers. a, RNA-seq over the course of ϕRR4 infection. Wild-type *L. ivanovii* RR3 was infected with ϕRR4 at an MOI of 1 and samples were collected for transcriptomic analysis by paired-end RNA-seq at the indicated time points. Reads were mapped to the ϕRR4 genome and normalized to the total reads per sample. Orange, top strand; brown, bottom strand. Representative of two biological replicates. **b**, Spacer enrichment correlates with target transcription, with no additional protection conferred above a critical expression threshold. Spacer abundance in the library was assessed before infection as well as 5 h after infection with ϕRR4 at an MOI of 1. Spacer enrichment distributions are shown, with individual histograms representing different tiers of target transcript abundance for the corresponding protospacer.

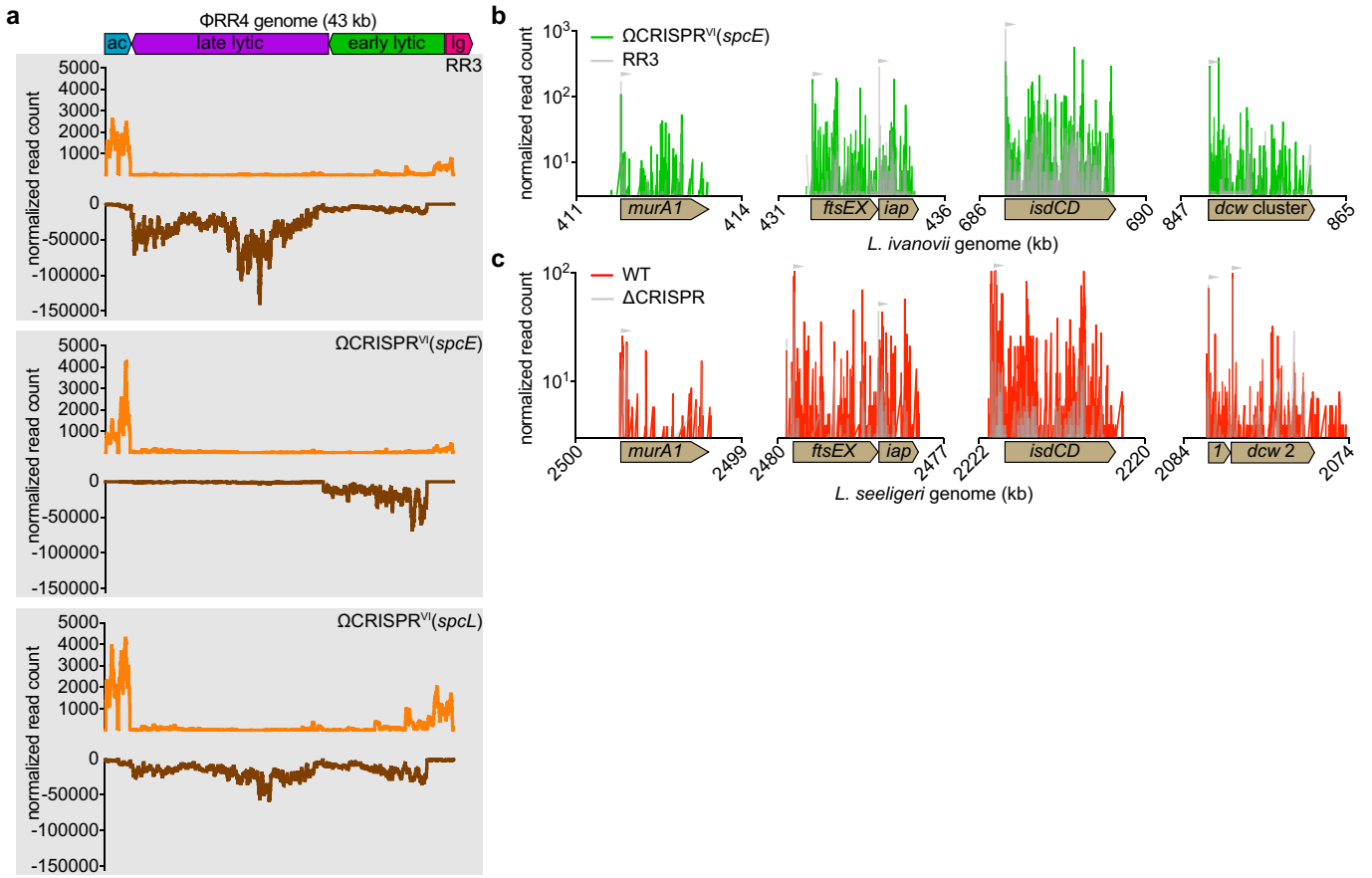

Extended Data Fig. 3 | Cas13a-mediated cleavage of phage and host transcripts detected by RNA-seq. a, Abundance of phage transcripts assessed by conventional paired-end RNA-seq 1.75 h after infection with ϕRR4 in *L. ivanovii* RR3 wild-type, ΩCRISPR^{VI}(*spcE*) or ΩCRISPR^{VI}(*spcL*) strains. Reads were mapped to the ϕRR4 genome and normalized to the abundance of a spike-in RNA. Both ΩCRISPR^{VI}(*spcE*) and ΩCRISPR^{VI}(*spcL*) targeting result in elevated early transcript cleavage products (Fig. 2a, b) and a reduction in late transcript abundance. Orange, top strand; brown, bottom strand. Representative of two biological replicates. **b**, *L. ivanovii* host mRNA cleavage detected by 5′ end mapping in *L. ivanovii* RR3 wild-type (grey) and ΩCRISPR^{VI}(*spcE*) (green) strains 1.75 h after infection with ϕRR4. The height of each peak represents the detected abundance of the corresponding mRNA 5′ end. Grey arrowheads, TSSs. Four regions of the genome are depicted: *murA1*, *ftsEX*/*iap*, *isdCD*, division and cell wall (*dcw*) cluster. Abundant intragenic cleavage products are generated in the ΩCRISPR^{VI}(*spcE*) strain. Representative of two biological replicates. **c**, The four genomic regions in **b** shown for the native type VI CRISPR host *L. seeligeri*, wild-type (red) and ΔCRISPR (grey), 15 min after aTc-mediated induction of a target transcript. The *dcw* cluster is broken into two operons in *L. seeligeri*. Representative of two biological replicates.

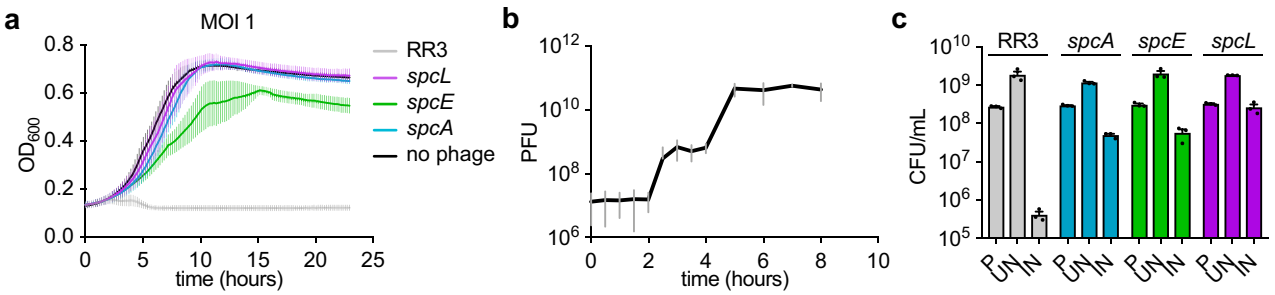

Extended Data Fig. 4 | *Trans*-RNase activity is sufficient to limit growth of both ϕRR4 phage and ΩCRISPR^{VI} host. a, *L. ivanovii* RR3 and ΩCRISPR^{VI}(*spcA*, *spcE* or *spcL*) strains at $OD_{600} = 0.05$ were infected with ϕRR4 at an MOI of 1 and growth was monitored over 24 h. Each curve represents the mean ± s.e.m. of three biological replicates. **b**, Quantification of ϕRR4 infective centres over time on wild-type *L. ivanovii* RR3. Cells were infected with ϕRR4 at an MOI of 0.1 and allowed to adsorb for 5 min, and then cells were washed three times to remove free phage. Infective centres were counted every 30 min by counting plaque-forming units on a lawn of phage-susceptible RR3 cells. Each data point represents the mean ± s.e.m. of three biological replicates. **c**, Survival of the indicated strains during ϕRR4 infection at an MOI of 2. CFU titres were measured before infection (P) and 4 h after infection (IN) or mock infection (UN). Each bar represents the mean ± s.e.m. of three biological replicates.

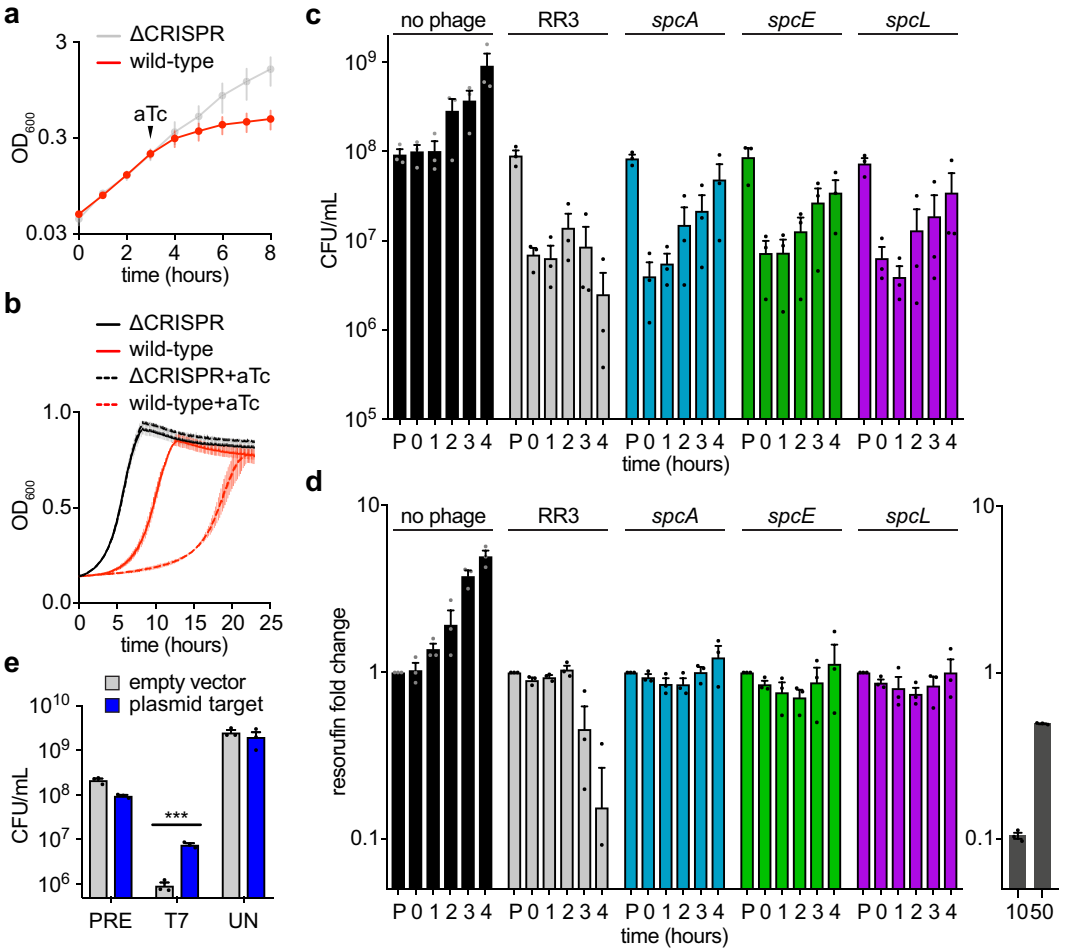

Extended Data Fig. 5 | Activation of Cas13a induces reversible dormancy of host cells. a, Growth arrest (measured as culture OD_{600}) induced by target transcription in wild-type *L. seeligeri* (but not the ΔCRISPR mutant) harbouring an aTc-inducible protospacer RNA. Arrowhead indicates addition of 100 ng ml^{-1} aTc. Each data point represents the mean ± s.e.m. of three biological replicates. **b**, Wild-type and ΔCRISPR *L. seeligeri* cultures carrying an aTc-inducible target transcript were exposed to 100 ng ml^{-1} aTc for 3 h as in **a**, then diluted (at time 0 h) to $OD_{600} = 0.05$ in fresh medium in the presence or absence of aTc, and growth was monitored over 24 h. Each curve represents the mean ± s.e.m. of three biological replicates. **c**, Immediate reduction in CFU upon phage infection of *L. ivanovii* RR3 or ΩCRISPR^{VI} strains. The indicated strains were infected with ϕRR4 at an MOI of 2, and CFU titres in the infected cultures were monitored over time. Pre-infection (P) and mock-infection titres were also measured. Each bar represents the mean ± s.e.m. of three biological replicates. **d**, Cell vitality within ΩCRISPR^{VI} cultures during phage infection. Cell vitality was measured in samples of cultures from **c** by monitoring conversion of nonfluorescent resazurin to fluorescent resorufin at each time point. The resorufin signal from heat-killed cells was subtracted from all samples as background, and each signal was normalized to the pre-infection value. Live cell standards (10% and 50%, mixed with heat-killed cells) are shown to demonstrate the quantitative capability of the vitality assay. Each bar represents the mean ± s.e.m. of three biological replicates. **e**, Phage-susceptible *L. ivanovii* ΩCRISPR^{VI}(*spcP*) cells harbouring a spacer against an aTc-inducible plasmid target RNA (or empty vector control) were treated with aTc for 1 h to pre-activate Cas13a, then infected with ϕRR4 at an MOI of 1. Viable CFUs were counted before infection (PRE), 7 h after infection (T7) or after mock infection (UN). Two-sided Student's *t*-test, $***P = 0.0005$. Each bar represents the mean ± s.e.m. of three biological replicates.

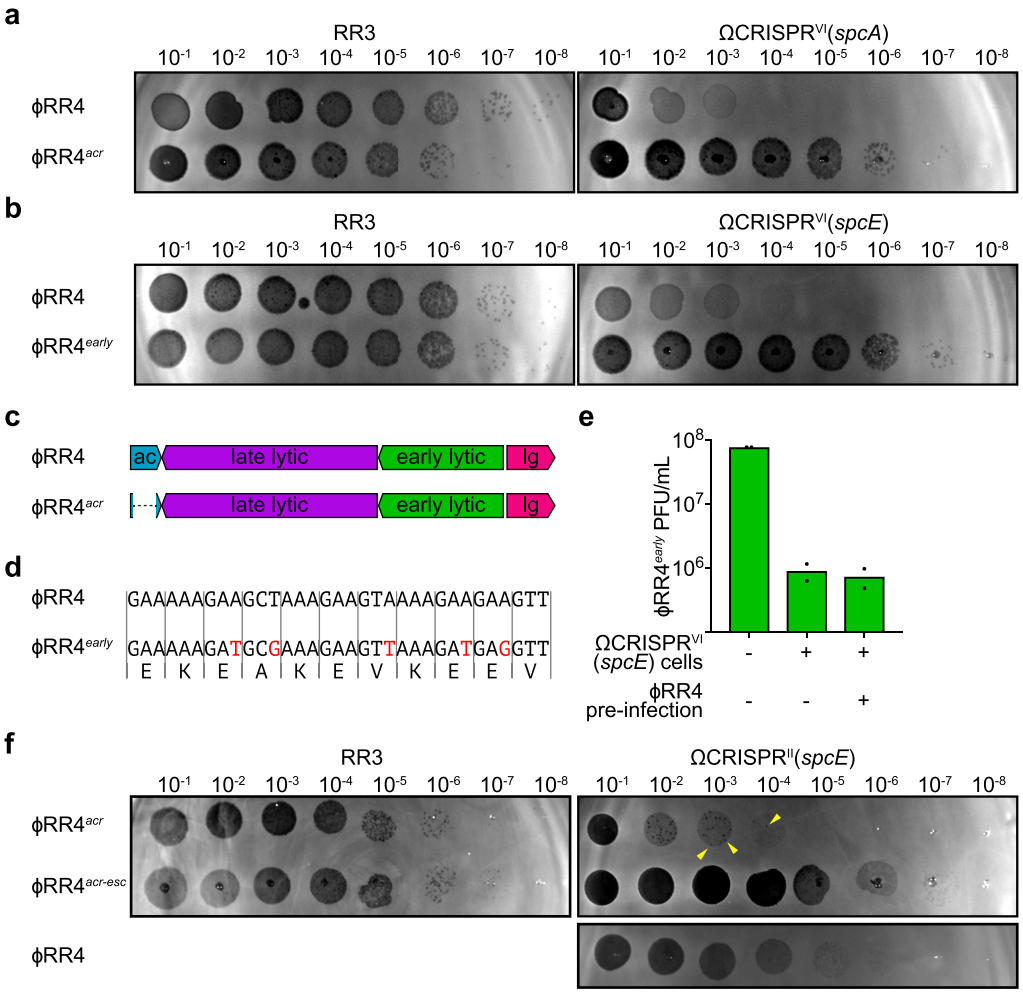

Extended Data Fig. 6 | Absence of CRISPR-resistant escape mutants and validation of engineered escaper phage. a, Efficiency of plaque-forming assays with wild-type ϕRR4 and engineered *spcA*-escaper phage ϕRR4^{acr} infecting *L. ivanovii* RR3 and ΩCRISPR^{VI}(*spcA*) strains. Phages were diluted and spotted onto top agar lawns containing the indicated strain. Escaper plaques were not observed in the presence of type VI CRISPR targeting. The ϕRR4^{acr} mutant, which lacks the *acr* region targeted by *spcA*, is viable and evades CRISPR targeting. Representative of two biological replicates. **b**, As in **a**, but testing the *spcE*-escaper phage ϕRR4^{early} and the ΩCRISPR^{VI}(*spcE*) strain. Representative of two biological replicates. **c**, Design of the ϕRR4^{acr} mutant, harbouring a deletion of the putative anti-CRISPR genes of ϕRR4. **d**, Design of the ϕRR4^{early} mutant, depicting the wild-type and mutant *spcE* target sequence. **e**, Cells pre-infected with wild-type ϕRR4 continue to adsorb escaper phage 2 h after infection. ΩCRISPR^{VI}(*spcE*) cells were infected with wild-type ϕRR4 at an MOI of 5 for 2 h (an uninfected control is shown for comparison), then washed three times with fresh medium to remove free phages. ϕRR4^{early} was added to cells (or to a cell-free control) at an MOI of 0.1 for 5 min, cells and bound phage were pelleted, and free phage in the supernatant were quantified as PFUs on a lawn of ΩCRISPR^{VI}(*spcE*) cells. Mean PFU values are shown from two biological replicates. **f**, Efficiency of plaque-forming assay using RR3 and ΩCRISPR^{II}(*spcE*) strains. We generated a ΩCRISPR^{II}(*spcE*) strain carrying the type II-A CRISPR system from *S. pyogenes* programmed with *spcE* against ϕRR4. This strain has very limited immunity to wild-type ϕRR4, but is highly immune to the ϕRR4^{acr} mutant, which lacks anti-CRISPR–Cas9 genes. Cas9-resistant ϕRR4^{acr} escaper plaques are evident in the plaque assay (yellow arrowheads). One escaper, ϕRR4$^{acr\text{-}esc}$, was isolated and confirmed to be resistant to Cas9 targeting. Representative of two biological replicates

nature research

Corresponding author(s): Luciano Marraffini

Last updated by author(s): Apr 15, 2019

Reporting Summary

Nature Research wishes to improve the reproducibility of the work that we publish. This form provides structure for consistency and transparency in reporting. For further information on Nature Research policies, see Authors & Referees and the Editorial Policy Checklist.

Statistics

For all statistical analyses, confirm that the following items are present in the figure legend, table legend, main text, or Methods section.

n/a	Confirmed
☐	☒ The exact sample size (*n*) for each experimental group/condition, given as a discrete number and unit of measurement
☐	☒ A statement on whether measurements were taken from distinct samples or whether the same sample was measured repeatedly
☐	☒ The statistical test(s) used AND whether they are one- or two-sided *Only common tests should be described solely by name; describe more complex techniques in the Methods section.*
☒	☐ A description of all covariates tested
☒	☐ A description of any assumptions or corrections, such as tests of normality and adjustment for multiple comparisons
☐	☒ A full description of the statistical parameters including central tendency (e.g. means) or other basic estimates (e.g. regression coefficient) AND variation (e.g. standard deviation) or associated estimates of uncertainty (e.g. confidence intervals)
☐	☒ For null hypothesis testing, the test statistic (e.g. *F*, *t*, *r*) with confidence intervals, effect sizes, degrees of freedom and *P* value noted *Give P values as exact values whenever suitable.*
☒	☐ For Bayesian analysis, information on the choice of priors and Markov chain Monte Carlo settings
☒	☐ For hierarchical and complex designs, identification of the appropriate level for tests and full reporting of outcomes
☒	☐ Estimates of effect sizes (e.g. Cohen's *d*, Pearson's *r*), indicating how they were calculated

Our web collection on statistics for biologists contains articles on many of the points above.

Software and code

Policy information about availability of computer code

Data collection	Genome sequencing, spacer library sequencing, and transcript 5' end mapping data were collected using Illumina MiSeq Control Software v2.6.2.1 Conventional RNA-seq data was collected using Illumina NextSeq 500 Control Software v4.0 qPCR data in Figure 3a was collected using Applied Biosystems QuantStudio 12k flex Growth curve data in Figs 3b, Extended Data 4b and 5b were collected with Tecan i-control v2.0 Resorufin fluorescence data in Extended Data 5d were collected with Tecan i-control v2.0
Data analysis	For genome sequencing: Reads were quality-trimmed using Sickle (https://github.com/najoshi/sickle) Reads were assembled into contigs using Abyss (https://github.com/bcgsc/abyss) Contigs were mapped to reference L. seeligeri and L. ivanovii genomes using Medusa (http://combo.dbe.unifi.it/medusa) Spacer library analysis: Spacer reads were mapped to the phage genome using bowtie2 (http://bowtie-bio.sourceforge.net/bowtie2/index.shtml) Custom Perl scripts were used to normalize spacer read counts, filter spacers containing fewer than 10 reads (pre-infection), and calculate enrichment ratios. These scripts are available upon request, as mentioned in the Code Availability statement below (and in the Methods section). RNA-seq analysis: RNA-seq reads (both conventional and 5' end mapping) were mapped to the host and phage genomes using bowtie2 (http://bowtiebio.sourceforge.net/bowtie2/index.shtml) Custom Perl scripts were used to designate transcriptional start sites, count transcript 5' ends within and downstream of the transcriptional start sites, filter trancripts containing fewer than 20 reads, and calculate corresponding cleavage ratios for each transcript. These scripts are available upon request, as mentioned in the Code Availability statement below (and in the Methods section).

Code Availability statement: Custom scripts used in analysis of spacer library data as well as RNA 5' end mapping data are available upon request.

For manuscripts utilizing custom algorithms or software that are central to the research but not yet described in published literature, software must be made available to editors/reviewers. We strongly encourage code deposition in a community repository (e.g. GitHub). See the Nature Research guidelines for submitting code & software for further information.

Data

Policy information about availability of data

All manuscripts must include a data availability statement. This statement should provide the following information, where applicable:

- Accession codes, unique identifiers, or web links for publicly available datasets
- A list of figures that have associated raw data
- A description of any restrictions on data availability

The L. seeligeri RR4 and L. ivanovii RR3 genome sequences, along with raw reads from the spacer library deep sequencing, paired end RNA-seq, and 5' end mapping have been deposited in the Sequence Read Archive under BioProject accession number PRJNA512236. Lists of strains, plasmids, and oligonucleotides used in this study are available in Supplementary Information 5.

Field-specific reporting

Please select the one below that is the best fit for your research. If you are not sure, read the appropriate sections before making your selection.

☒ Life sciences ☐ Behavioural & social sciences ☐ Ecological, evolutionary & environmental sciences

For a reference copy of the document with all sections, see nature.com/documents/nr-reporting-summary-flat.pdf

Life sciences study design

All studies must disclose on these points even when the disclosure is negative.

Sample size	No sample size calculation was performed. All experiments were performed with sample sizes based on standard protocols in the field.
Data exclusions	In spacer library analysis, spacers with fewer than 10 reads (pre-infection) were discarded to reduce noise and report accurate enrichment values. For transcript 5' end analysis, the transcriptional start sites could not be accurately determined for transcripts with fewer than 20 reads, therefore these data were excluded from analysis.
Replication	All measurements of phage infection efficiency, phage DNA content, and cell survival were performed in at least biological triplicate. NGS experiments were performed in biological duplicates.
Randomization	n/a. Animal or human research subjects were not involved in this study. None of the experiments were randomized.
Blinding	n/a. Animal or human research subjects were not involved in this study. None of the investigators were blinded.

Reporting for specific materials, systems and methods

We require information from authors about some types of materials, experimental systems and methods used in many studies. Here, indicate whether each material, system or method listed is relevant to your study. If you are not sure if a list item applies to your research, read the appropriate section before selecting a response.

Materials & experimental systems

n/a	Involved in the study
☒	☐ Antibodies
☒	☐ Eukaryotic cell lines
☒	☐ Palaeontology
☒	☐ Animals and other organisms
☒	☐ Human research participants
☒	☐ Clinical data

Methods

n/a	Involved in the study
☒	☐ ChIP-seq
☒	☐ Flow cytometry
☒	☐ MRI-based neuroimaging